



Energy harvesting from different aeroelastic instabilities of a square cylinder



Thomas Andrianne^{a,*}, Renar P. Aryoputro^a, Philippe Laurent^b, Gérald Colson^b,
Xavier Amandolèse^{c,d}, Pascal Hémon^c

^a Department of Aerospace and Mechanical Engineering, University of Liège, Allée de la Découverte, 9 Quartier Polytech 1, B52/3, B-4000 Liège, Belgium

^b Department of Electrical Engineering and Computer Science, University of Liège, Allée de la Découverte, 10 Quartier Polytech 1, B28, B-4000 Liège, Belgium

^c LadHyX, UMR 7646, CNRS-Ecole Polytechnique, F-91128 Palaiseau, France

^d Conservatoire National des Arts et Métiers, F-75141 Paris, France

ARTICLE INFO

Keywords:

Energy harvesting
Aeroelasticity
Galloping
Vortex-induced-vibration
Wind tunnel
Modelling

ABSTRACT

This paper presents an experimental and numerical investigation of the power extraction from the oscillations of a square beam due to aeroelastic instabilities. The energy harvesting is performed using a coil-magnet arrangement connected to a variable resistance load with the target objective to auto-power a remote sensor. Two aeroelastic phenomena are investigated: Vortex Induced Vibration (VIV) and cross-flow galloping. The first instability (VIV) is analyzed on a free-standing vertical structure. A second experimental set-up is developed on a horizontal square cylinder supported by springs, free to oscillate vertically as a rigid body. In this case, both galloping and VIV interact, leading to interesting characteristics in order to harvest energy from the wind. The behavior of each electro-mechanical aeroelastic system is investigated for different reduced wind speeds and load resistances in a wind tunnel. Observed efficiencies are rather low, but large enough to power a remote sensor with an adapted measuring strategy. Both harvesting systems are then studied numerically using a wake oscillator model (for VIV) coupled to a quasi-steady model (for galloping) and an electric model (for the harvester). This mathematical model is used to extend the parametric space and to highlight the effectiveness of the high stable branch of the VIV-galloping curve to harvest energy.

1. Introduction

The amount of smart remote sensors has constantly increased over the last years. The objective of such sensors is to obtain information about the environment (temperature, luminosity, noise, humidity, ...) or to take part to communication networks. A main drawback of such systems is the need to supply power: conventional power supplies, such as battery or supply cables, consist in the main obstacle to reach a higher integration of microsystems in engineering applications. The energy harvesting concept can relax this constrain by using free and renewable energy to power ultra-low power devices.

The objective of this work is to study the potential of simple aeroelastic systems to harvest energy from the wind. One of the difficulty concerns the coupling of the harvesting device to the aeroelastic system, which might change the behavior of the global electro-aeroelastic model. Many research works have been dedicated to this topic. Some of them are purely experimental (Sousa et al., 2011; Hémon et al., 2017; Bernitsas et al., 2008), numerical (Tang et al., 2009; Vicente-Ludlam et al., 2014) or in-between, without modelling the harvester (Barrero-Gil et al., 2012).

In the scope of this work, we first focus on an experimental investigation on two types of aeroelastic phenomena: (i) VIV of a vertical structure and (ii) VIV-galloping of a horizontal structure. A full electro-aeroelastic model is then used to push further the analysis by expanding the parameter space and discussing the corresponding energy harvesting possibilities.

2. Methodology

For each configuration, a wind tunnel test campaign is carried out to measure the amplitude of motion and the electrical power (P_{EH}) as a function of the reduced velocity, for different values of the load resistance of the harvesting device. In parallel, the electro-aeroelastic behavior is investigated by adequate numerical models: For VIV, the model proposed by Tamura (Tamura and Matsui, 1979) is selected. This model is a wake oscillator type (two degrees of freedom), having the advantage to involve parameters that can be related to static aerodynamic quantities. For galloping, the classical Parkinson's model using a fifth order polynomial form of the vertical force coefficient is selected

* Corresponding author.

E-mail address: t.andrianne@uliege.be (T. Andrianne).

(Parkinson and Smith, 1964). The empirical constants of this model are taken from the works of Nakamura (Nakamura and Mizota, 1975).

These non-linear models allow to capture the complex aeroelastic behavior of the systems (lock-in for VIV and subcritical bifurcation for galloping). In the case of the horizontal beam, where VIV and galloping are expected to interact, the two models are coupled to reproduce this interaction effect, which changes the form of the traditional bifurcation diagram (Mannini et al., 2014). The models are used to quantify the potential energy transfer between the flow and the structure. Barrero et al (Barrero-Gil et al., 2012) and Vicente-Ludlam et al. (Vicente-Ludlam et al., 2014) proposed a similar approach using fluid force models based on experimental data.

3. Wind tunnel models

The tests are performed in the multi-disciplinary wind tunnel of University of Liège, in uniform low turbulence flow conditions (TI<0.2%). Two experimental apparatus are used in this study: a vertical set-up (Fig. 1) and a horizontal set-up (Fig. 2). The set-ups consist of square aluminium tube with a side of 50 mm (noted D), a thickness of 2 mm and a length of 1650 mm and 1340 mm for the vertical and horizontal apparatus respectively. The beam is simply clamped on the floor of the test section in the case of the vertical set-up, resulting in a cantilever beam. For the second set-up, the beam is supported horizontally by two thin rectangular beams, playing the role of springs. In this case the motion of the square cylinder is purely vertical thanks to the important length of the spring beams. The harvesting device consists of a coil-magnet assembly mounted at the tip of the model for the vertical set-up (Fig. 1) and on one side of the model for the horizontal set-up (Fig. 2).

The structural characteristics of each set-up are identified through free responses (hammer impacts) imposed to the beam (see Table 1). A laser displacement sensor is used to measure the motion of the model. A variable load resistance is connected to the coil-magnet device. A voltmeter measures the voltage through the load resistance (V_L) and the electrical power produced by the harvesting system is calculated by $P_{EH} = V_L^2 / R_L$.

4. Experimental results

The VIV response and electrical power extracted by the coil-magnet assembly in the case of the vertical structure are presented in Fig. 3 as a function of the reduced velocity ($U^* = \frac{U}{fD}$) and for different values of the load resistance. It is observed that the VIV oscillations starts around $U^* \sim 7.7-1/0.13$ (shown as a grey square marker), where $St = 0.13$ is a good estimate of the Strouhal number of the square cylinder in this range of Reynolds number. The lock-in range is equal to $\Delta U^* = 2.5$, which is small because of the large value of the Scruton number of the system ($Sc = \frac{2\pi m_s}{\rho D^2} = 10.5$). The effect of the load resistance on the amplitude of

vibration and lock-in range is low.

The maximum electrical power is reached around $U^* \sim 8$ and for a load resistance around 400Ω . The optimum value of the load resistance matches the resistance of the coil ($R_C = 406\Omega$) in accordance with the Maximum Power Transfer Theorem.

Fig. 4 shows the galloping response and power output as a function of the reduced velocity for the horizontal set-up. In this figure the grey and black square markers correspond to the critical VIV velocity and the quasi-steady prediction of the galloping velocity respectively. The curve shows no clear VIV response. Instead, the galloping phenomenon is triggered by the VIV instability and the resulting bifurcation branch follows linearly the reduced velocity U^* . This close vicinity between the two critical velocities is interesting because the initiation of the vibration and hence energy production is less sensitive to the energy extraction.

It is observed that the load resistance has no effect on the resulting oscillation amplitude but a strong effect on the extracted power. The optimal value of the load resistance is $R_L = 255\Omega$, matching the internal resistance of the coil ($R_C = 257\Omega$), similarly to the case of the vertical set-up presented above.

Fig. 5 presents the efficiency (P_{EH}/P_{WIND}) in the plane (U^*, R_L). The wind power being defined by the kinetic energy flux of air passing through the area swept by the oscillating square cylinder. In the left plot, the VIV optimal efficiency is clearly localized on a peak, centered on (8,400). Beyond this peak ($U^* > 10$), no more energy can be extracted by the system since the lock-in phenomenon ended. In the right plot, the situation is different: beyond the critical velocity ($U^* = 10$), the system is unstable and energy can be harvested up to $U^* = 30$ (which is the limit of the wind tunnel test). Nevertheless, the optimum harvesting region lies around $U^* = 15$ and $R_L = 250\Omega$. This is a clear difference between the two harvesting apparatus.

On the energy harvesting point of view, the power outputs of the set-up are small but large enough to power small size sensors which are able to operate with 1 mW, with an adapted strategy. The efficiency is low: 10^{-6} for the VIV set-up and 10^{-3} for the VIV-galloping system. This result brings out the poor efficiency of the current design choice for the coil/magnet assemblies to harvest the mechanical energy of motion. The model presented in the next section will highlight possible improvements.

5. Modelling

A mathematical model of the energy harvesting system is built by coupling an electromechanical galloping system, as proposed by Vicente et al. (Mannini et al., 2014) to the vortex induced vibration model proposed by Tamura (Barrero-Gil et al., 2012). The model consists of three non-dimensional equations:

$$\ddot{Y} + \left(2 \zeta_s + \frac{n(f+D)v}{S_*} \right) \dot{Y} + Y = -\frac{fnv^2\theta}{S_*^2} \frac{F_Y}{M\omega^2 D} - \frac{k_E}{M\omega^2 D} I \quad (1)$$

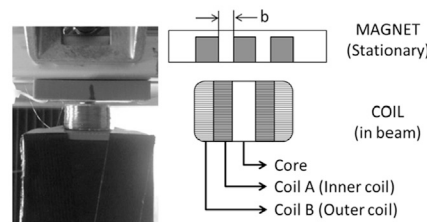


Fig. 1. Vertical experimental set-up installed in the test section (left) - Coil/magnet assembly (right).



Fig. 2. Horizontal set-up installed in the test section (left) - Coil/magnet assembly (right).

Table 1
Modal properties of the experimental set-up.

	f [Hz]	ζ [%]	m (kg/m)
Vertical set-up	17.0	0.5	1.03
Horizontal set-up	6.06	0.24	1.79

$$\ddot{\theta} - 2\eta\nu \left[1 - \frac{4f^2}{C_{L0}^2} \theta^2 \right] \dot{\theta} + \nu^2 \theta = -m_* \ddot{Y} - \nu S^* \dot{Y} \quad (2)$$

$$(R_C + R_L)I + L\omega \dot{I} = k_E \omega D \dot{Y} \quad (3)$$

, where equations (1)–(3) model respectively the vertical motion of the structure Y , the behavior of the wake θ , and the electric circuit associated with the harvesting device through the electric current I . In these equations, the dot symbol refers to the derivative relative to the non-dimensional time $\tau = \omega t$. The aerodynamic force F_Y appearing in equation (1) is classically expressed as a polynomial function of \dot{Y} , as proposed by Parkinson (Parkinson and Smith, 1964):

$$F_Y = nU^2 \left[A_1 \left(\frac{\dot{Y}}{U} \right) - A_2 \left(\frac{\dot{Y}}{U} \right)^3 + A_3 \left(\frac{\dot{Y}}{U} \right)^5 - A_4 \left(\frac{\dot{Y}}{U} \right)^7 \right] \quad (4)$$

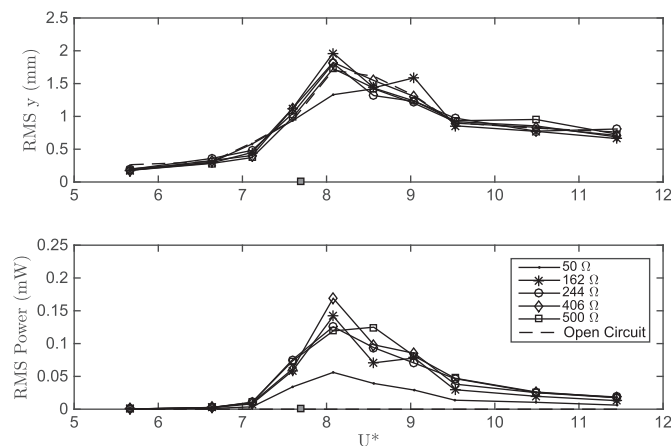


Fig. 3. Vertical set-up (VIV): Response and electrical power output vs. U^* , for different values of the load resistance.

The A_i 's coefficients can be found in Nakamura (Nakamura and Mizota, 1975) for the Reynolds number corresponding to the present experiments. The variable n corresponds the ratio of the mass of the structure to the mass of air ($n = \rho D^2 / 2m$, where m is the mass per unit span of the structure).

Equation (2) models the behavior of the wake, which is characterised by an alternate vortex shedding process. This non-linear equation is based on a Birkhoff's oscillator model, coupled to the equation of motion of the structure (equation (1)) through the velocity and acceleration. The non-linear feature of the equation leads to self-limited amplitude motion of both the structure and the wake, which is adapted to represent the VIV phenomenon. In this model, the variable ν corresponds to the ratio of the wind speed to the critical VIV velocity ($\nu = U/U_c$). The parameter f corresponds to the Magnus effect creating lift. In his work (Tamura and Matsui, 1979), Tamura proposed a value of $f = 1.16$ for a circular cylinder. Because of the important differences between the flow around a circular and a square cylinder, it is proposed here to vary this coefficient in order to fit the experimental response.

Another important parameter is the electromechanical coefficient k_E giving rise to the electromagnetic force induced by the coil-magnet arrangement on the structure: $F_{EM} = k_E I$.

Assuming a harmonic behavior, k_E can be computed as:

$$k_E = \frac{V_{RMS}}{Y_{RMS}} \frac{(1 + R_L/R_C)}{\omega} \sqrt{1 + \beta^2} \quad (5)$$

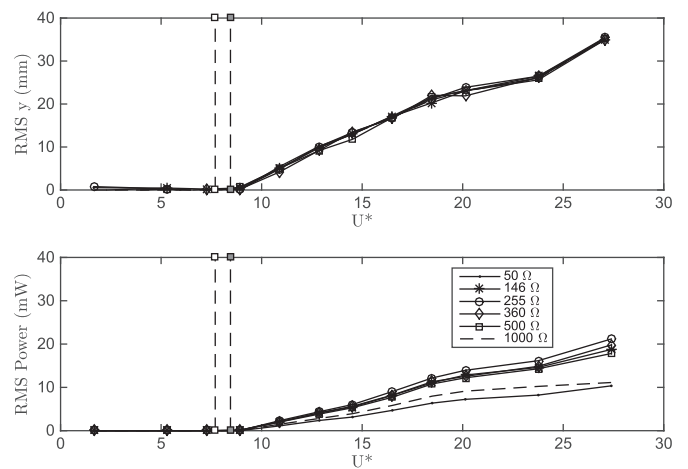


Fig. 4. Horizontal set-up (VIV-Galloping): Response and electrical Power output vs. U^* , for different values of the load resistance.

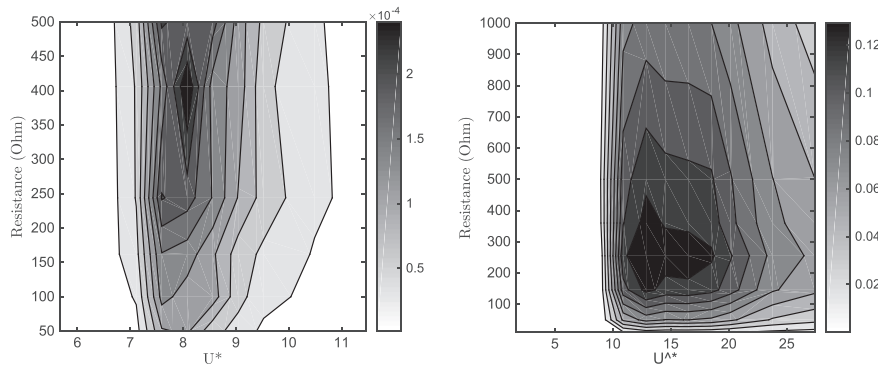


Fig. 5. Efficiency (in %) of the harvesting systems: Vertical set-up (left) and horizontal set-up (right).

Introducing a parameter $\beta = L\omega/(R_C + R_L)$ which characterises the ratio between the electrical and mechanical time periods. For low frequency oscillations, which is the case in the present experiments, the effect of the inductance on the overall dynamics can be neglected, i.e. $\beta \ll 1$, and the electromechanical model becomes

$$\ddot{Y} + \left(2\zeta_s + \frac{n(f+D)\nu}{S_*} \right) \dot{Y} + Y = -\frac{fn\nu^2\theta}{S_*^2} \frac{F_Y}{M\omega^2 D} - \frac{k_E^2}{M\omega(R_C + R_L)} \dot{Y} \quad (6)$$

$$I = \frac{k_E \omega D}{(R_C + R_L)} \dot{Y} \quad (7)$$

The electromagnetic force acting on the system can then be viewed as an added viscous damper for which an equivalent damping ratio can be defined as:

$$\zeta_E = \frac{k_E^2}{2 M \omega (R_C + R_L)}. \quad (8)$$

And equation (5) becomes

$$\ddot{Y} + \left[2(\zeta_s + \zeta_E) + \frac{n(f+D)\nu}{S_*} \right] \dot{Y} + Y = -\frac{fn\nu^2\theta}{S_*^2} \frac{F_Y}{M\omega^2 D} \quad (9)$$

Using the experimental measurement of voltage and displacement associated to Figs. 3 and 4, it is possible to quantify the value of the electromechanical coefficient (4) and equivalent damping ratio (8) for both VIV and VIV-galloping energy harvesting setups. Results are reported at their respective optimal resistance ($R_L = R_C = 406 \Omega$ for the

VIV set-up and $R_L = R_C = 255 \Omega$ for the VIV-galloping setup) in Figs. 6 and 7.

For both setups, the electromagnetic damping ratio is low in comparison with the structural damping ratio ($\zeta_s = 0.24\%$). It explains why the dynamical response is almost the same without and with the energy harvesting device (see Figs. 3 and 4).

For the galloping setup one can also notice that the electromechanical coefficient and thus the equivalent electromagnetic damping ratio decrease with the oscillation amplitude, which means that the efficiency of the harvesting device decreases with the oscillation amplitude.

6. Discussion

The complete electro-aeroelastic model associating both VIV and galloping equations is used here to study the effect of the electromechanical coefficient k_E on the electrical power and overall energy harvesting efficiency. As observed experimentally, the present coil-magnet arrangement doesn't affect the mechanical response and hence it is far from optimal because the added damping is one order of magnitude lower than the structural damping.

The horizontal set-up is selected here and the experimental results are compared to the numerical predictions. This set-up is chosen because of its larger efficiency and operational range in terms of reduced velocity.

As a validation step, the experimental measurements with no energy harvesting is performed, i.e. k_E is set to zero, are compared to the model predictions with or without the vortex induced vibration part. When including the VIV formulation the model is called 'Tamura-Parkinson' (TP). Excluding it, the model is referred as 'Parkinson'. Fig. 8 shows the non-dimensional response amplitude versus reduced velocity. The lower limit cycle oscillations (LCO) branch obtained from Parkinson model

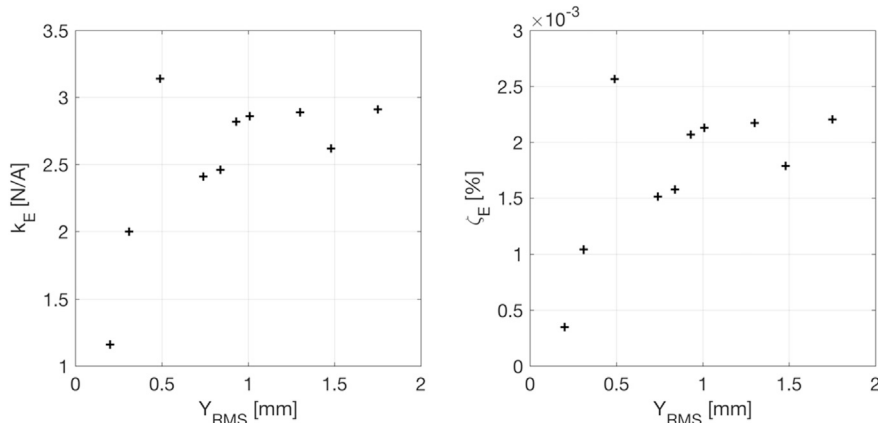


Fig. 6. Evolution of the electromechanical coefficient k_E and equivalent damping ratio ζ_E with the amplitude of oscillations; VIV energy harvesting set-up for $R_C = 406 \Omega$.

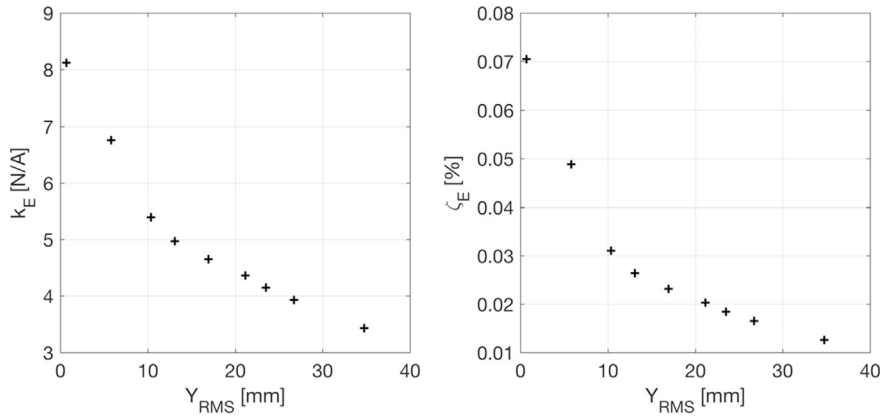


Fig. 7. Evolution of the electromechanical coefficient k_E and equivalent damping ratio ζ_E with the amplitude of oscillations; Galloping energy harvesting set-up for $R_C = 255 \Omega$.

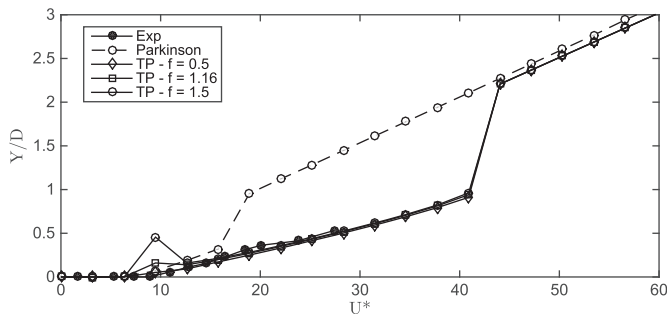


Fig. 8. Aeroelastic response of the horizontal set-up vs. reduced velocity for $k_E = 0$. Comparison of experimental and numerical results: Parkinson and Tamura-Parkinson (TP).

matches the experimental results but with an overestimation of the slope. More importantly, the model predicts a jump to the high LCO galloping branch for $U^* \sim 15$, which was not observed experimentally. This single experimental branch could be either explained by the presence of a structural nonlinearity in the experimental system or, because the maximum wind speed tested was too low. This second assumption is supported by the results of the Tamura-Parkinson model in Fig. 8. Indeed, this model captures correctly the linear evolution of the response with the reduced velocity. Nevertheless, it overestimates the amplitude of the VIV response around $U^* = 8$. By decreasing the value of the parameter f , the effect of vortex shedding and hence the VIV response are reduced. The non-synchronous characteristic of vortex shedding process along the

span of the square model could justify the need to reduce the value of f .

Though not observed experimentally, the higher branch of the response is obtained from the mathematical models. The potential of energy harvesting from this branch is high thanks to the large amplitude and hence its high energy content.

With an energy harvesting device ($k_E > 0$) and under the assumption of $\beta \ll 1$, the electrical power extracted from the coil-magnet system can be directly computed from the dynamical response of the setup:

$$P_E = R I_{RMS}^2 \approx \frac{1}{R_L} \left(\frac{k_E \omega_s}{1 + R_C/R_L} \right)^2 Y_{RMS}^2 \quad (10)$$

And the system efficiency can be computed from the ratio of the electric power to the wind power, i.e. the kinetic energy flux of air passing through the area swept by the oscillating beam:

$$\eta_E = \frac{P_E}{\frac{1}{2} \rho U^3 s D (1 + 2Y_{RMS})} \quad (11)$$

The complete electromechanical model is used to calculate the value of Y_{RMS} for different values of k_E in the range of reduced velocity U^* spanning from 0 to 120.

Fig. 9 shows the effect of k_E when both resistances are equal ($R_L = R_C = 255 \Omega$), leading to the optimal electric configuration. The variation of k_E between 0 and 15, while keeping the other parameters constant, corresponds to an increase of the electromechanical damping ζ_E from 0% to 0.24%. Hence it doubles the total damping of the system at wind off condition, i.e. without positive or negative aerodynamic damping.

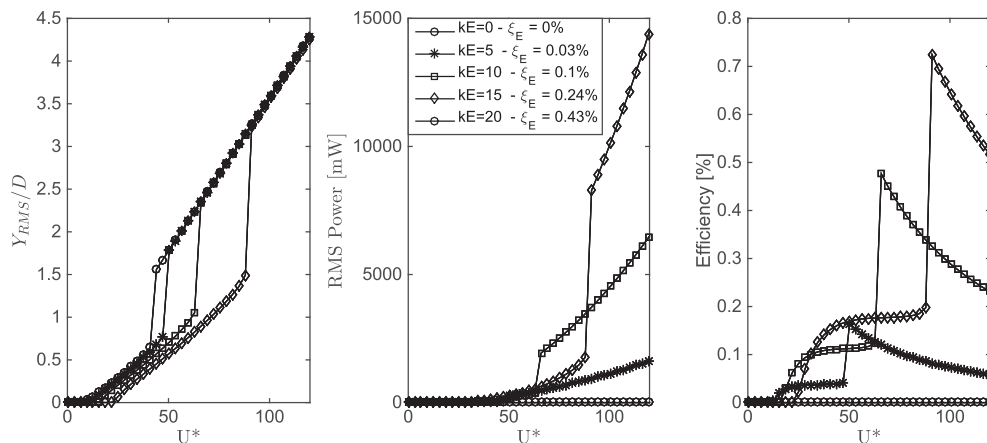


Fig. 9. Evolution of the relative displacement, extracted power and efficiency with the reduced velocity for various electromechanical coefficient k_E up to 16; VIV-Galloping (Tamura-Parkinson) energy harvesting model, $R_C = R_L = 255 \Omega$.

As expected, the effect on the aeroelastic response is to shift the lower branch to the right: the critical reduced velocity increases if energy is extracted from the system. On the other hand, the amplitude of the higher branch of the galloping response is unaffected by the added damping: once the system jumps on the higher branch the energy harvesting does not impact its motion because it is located on a strong stable limit cycle oscillation regime. For all values of the electromechanical coefficient, a large amount of power can be extracted from this higher branch (central plot of Fig. 9). There is a factor of four in comparison with the power available from the lower branches. Finally, the right plot of Fig. 9 shows that the efficiency in the higher branch decreases inversely to the reduced velocity, due to the increase of the area spanned by the oscillating structure. For the optimal reduced velocity, tripling the electromechanical coefficient and hence damping leads to an increase of efficiency by a factor of 10. Note that the efficiency of the lower branch is also impacted by the increase of k_E . In this case, tripling the electromechanical coefficient leads to an increase of efficiency by a factor of 5.

As a conclusion, the harvester must be designed in order to maximise the value of k_E , while adapting the modal parameters of the system (frequency and mass) in order to stay on the stable lower branch or to catch the higher one in the range of frequent wind speeds. Note that the lower branch has the advantage to be horizontal, ensuring a constant efficiency over a large range of reduced velocities.

7. Conclusions

The present work investigates the potential of energy harvesting from the VIV and galloping phenomena of a square cylinder in an airflow. Experimental results are presented and the electrical power output is shown for the two tested configurations (vertical and horizontal set-up). As expected, the global efficiencies values (P_{EH}/P_{WIND}) are very low: $10^{-4}\%$ for VIV and 0.1% for VIV-galloping. Nevertheless the power output (~ 0.15 mW for VIV and ~ 15 mW for VIV-galloping) are sufficient to power sensors with an adapted strategy. Numerical models are used to

capture the complete aeroelastic/electromechanical behavior of the system. Results showed that a VIV-galloping model coupled with the electromechanical model allows to reproduce the behavior of the horizontal set-up. Under the assumption of low inductance of the coil-magnet assembly, the effect of the electromechanical coupling is simplified into added damping. The resulting model is used to draw some conclusions about the effect of extracting energy from the system. The main conclusion concerns the higher branch of the VIV-galloping curve, which has a large potential for energy harvesting because of its high energy content and stability.

References

- Barrero-Gil, A., Pindado, S., Avila, S., 2012. Extracting energy from Vortex-Induced Vibrations: a parametric study. *Appl. Math. Model.* 36 (7), 3153–3160.
- Bernitsas, M.M., Raghavan, K., Ben-Simon, Y., Garcia, E.M., 2008. VIVACE (vortex induced vibration aquatic clean energy): a new concept in generation of clean and renewable energy from fluid flow. *J. Offshore Mech. Arct. Eng. ASME Trans.* 130, 041101.
- Hémon, P., Amandolese, X., Andrianne, T., 2017. Energy harvesting from galloping of prisms: a wind tunnel experiment. *J. Fluids Struct.* 70, 390–402.
- Mannini, C., Marra, A.M., Bartoli, G., 2014. VIV-galloping instability of rectangular cylinders: review and new experiments. *J. Wind Eng. Ind. Aerod.* 132, 109–124.
- Nakamura, Y., Mizota, T., 1975. Torsional flutter of rectangular prisms, *Journal of the engineering mechanics division. ASCE* 101 (EM2), 125–142.
- Parkinson, G.V., Smith, J.D., 1964. The square prism as an aeroelastic non-linear oscillator. *Q. J. Mech. Appl. Math.* XVII, 225–239.
- Sousa, V.C., Anicezio, M. de M., De Marqui Jr., C., Erturket, A., 2011. Enhanced Aeroelastic Energy Harvesting by Exploiting Combined Nonlinearities: theory and Experiment. *Smart Mater. Struct.* 20 <https://doi.org/10.1088/0964-1726/20/9/094007>.
- Tamura, Y., Matsui, G., July 1979. Wake-oscillator model of vortex-induced oscillation of a circular cylinder. In: *Proceedings of the 5th International Conference on Wind Engineering*, vol. 2, pp. 1085–1092. Fort Collins, Colorado, USA.
- Tang, L., Païdoussis, M.P., Jian, J., 2009. Cantilevered flexible plates in axial flow: energy transfer and the concept of flutter-mill. *J. Sound Vib.* 326, 263–276.
- Vicente-Ludlam, D., Barrero-Gil, A., Velazquez, A., 2014. Optimal electromagnetic energy extraction from transverse galloping. *J. Fluids Struct.* 51, 281–291.